Project No. 037005

CECILIA

Central and Eastern Europe Climate Change Impact and Vulnerability Assessment

Specific targeted research project

1.1.6.3.I.3.2: Climate change impacts in central-eastern Europe

D3.4: Climate change scenarios for near future (time slice 2020-2050)

Due date of deliverable: 1st February 2009
Actual submission date: 1st October 2009

Start date of project: 1st June 2006 **Duration: 36 months**

Lead contractor for this deliverable: National Meteorological Administration (NMA)

Project co-funded by the European Commission within the Sixth Framework Programme (2002-2006)		
Dissemination Level		
PU	Public	X
PP	Restricted to other programme participants (including the Commission Services)	
RE	Restricted to a group specified by the consortium (including the Commission Services)	
CO	Confidential, only for members of the consortium (including the Commission Services)	

Contributing partners: IAP, CUNI, NMA, ELU

1. Introductory remarks

The goal of this deliverable is to construct climate change scenarios for the near future (2021-2050) for various Central and South-European areas using statistical downscaling methods (SDS). The contributions of partners to this deliverable refer mainly to the following techniques: 1) statistical downscaling models based on statistical relationships between local predictands and large-scale predictors (NMA, ELU, IAP), calibrated on observed data set and then applied to predictors simulated by the global models (GCMs); 2) postprocessing procedures of the target variables derived directly from regional climate models (RCMs), correcting for systematic errors in the statistical distribution of the target variables (CUNI). More details regarding the validation of these statistical methods are presented in the CECILIA deliverable D3.3.

A single GCM/RCM or more (ensemble) GCMs have been used as drivers in the statistical downscaling models. The second option allows having a better evaluation of the uncertainties associated to the statistical downscaled estimations. In addition to this, a comparison with the results obtained by dynamical downscaling is also presented. Details about the results obtained by each partner involved in this deliverable are presented in the following and a synthesis about the methodologies is presented in Table 1.

Table1. Information on the statistical downscaling techniques used in this study.

Participant ID Responsible person	SDS methodology	SDS input	SDS output: parameter, grid or stations	SDS domain
IAP Martin Dubrovsky	Stochastic weather generator (i) Delta approach (ii) Pattern scaling	11 GCMs from MAGIC	Monthly temperature and precipitation total (1 station: Prague)	1 station: Prague
CUNI Jiri Miksovsky	Dynamical-empirical	ECHAM-RegCM	T_{max}, T_{min}, precipitation (daily); 832 grid points	CECILIA common domain
NMA Aristita Busuioc	Statistical-based on CCA	8 ENSEMBLES-GCMs (stream1), +ARPEGE	Monthly temperature (94 stations) and precipitation total (16 stations)	LON:20-30°E, LAT:43-50°N (temperature), LON:24-27°E LAT:43-45°N (precipitation)
ELU Judit Bartholy	Stochastic	AT-700 hPa (2,5°)	Temperature, precipitation (1° resolution grid)	LON: 16-23°E LAT: 46-49°N

2. IAP contribution

2.1 Introduction

The input weather series for agricultural and hydrological climate change impact experiments in Czechia were mostly prepared by the stochastic weather generator Met&Roll (Dubrovský et al., 2000; Dubrovský et al., 2004), whose parameters were modified according to the climate change scenarios derived from GCM simulations. Two approaches were used to derive the climate change scenarios at the Prague station from the GCM simulations: Delta approach and the Pattern scaling. The Delta approach was used to derive the scenarios from the daily GCM outputs. As these are available only for shorter time slices, it was applied only for the time slice 2081-2100. More details are presented in the CECILIA deliverable D3.5. The pattern scaling method, which is the preferred method, was used when the scenarios were derived from the monthly GCM outputs, which is available for much longer periods compared to the daily outputs. The results based on this approach corresponding to the years 2025 and 2050 are presented in this deliverable.

2.2 Scenarios derived by the pattern scaling method from the monthly GCM outputs

The "Pattern Scaling" method (Dubrovsky et al., 2005) is based on an assumption that the change of each climatic characteristic ΔX is linearly proportional to the change in global mean temperature ΔT_G:

$$\Delta X = \Delta X^* \times \Delta T_G$$

where ΔX^* is the standardised change of X related to 1 degree rise in global mean temperature. The set of standardised changes of all relevant climatic characteristics and for all month is then called the standardised climate change scenario. In our case, the relevant climatic characteristics are: daily average and extreme temperatures, daily precipitation sum and daily global solar radiation. Humidity and wind speed, which are also needed for some impact models, are added by the resampling method because of the incompleteness of the GCM databases. The scenarios derived from the monthly GCM outputs include changes in the means and standard deviations of monthly values of individual climatic characteristics. The changes in temperature means are given in terms of Celsius degrees, changes in all other climatic characteristics (including standard deviations of monthly temperatures) are given in terms of percentage.

Advantages of the pattern scaling method include: (i) the standardised scenarios may be derived (using the linear regression) from a long GCM-simulated time slice (e.g. 1961-2100) which implies a lower sampling error and thereby higher robustness of the scenarios (compared to the Delta approach commonly applied to shorter time slices). (ii) The change in global mean temperature, ΔT_G, which is used to scale the standardised scenarios may be estimated by a simpler (compared to GCM) one-dimensional energy-balance model MAGICC (Harvey et al. 1997, Hulme et al. 2000; http://www.cgd.ucar.edu/cas/wigley/magicc/), which models evolution of the global temperature in response to chosen emission scenario, climate sensitivity and several other model parameters. This approach allows scaling of the standardised scenarios derived from GCMs run at a single emission scenario for a set of user-selected combinations of emission scenario and climate sensitivity. In result, by using a set of standardised scenarios derived from several GCMs scaled by a suitably selected set of values of the scaling factor (ΔT_G), the pattern scaling method allows to effectively account for uncertainties in these two major driving constraints. The use of the pattern scaling method thus allows to bypass the two shortcomings of the available set of GCM simulations: (i) The outputs from existing GCM simulations (Fig.2.1) show, that the ΔT_G projections till 2100 based on available GCM set do not account for the uncertainty in climate sensitivity (which is a topic of broad scientific discussions). (ii) The GCM database does not include all 4 markers emission scenarios in individual GCMs.

Construction of the standardised scenarios: The standardised scenarios are derived from the GCM-simulated time series of monthly averages of climatic characteristics using a linear regression, in which the global mean temperature is the independent variable, and the respective climatic characteristic is a dependent variable. The standardised scenarios for the CECILIA project were derived from the most recent GCM simulations (SRES-A2 emission scenario) made for the IPCC 4th Assessment Report (IPCC, 2007). Specifically, SRES-A2 runs were used. This emission scenario

assumes the highest GHG emissions of the four marker emission scenarios, so that it implies highest signal-to-noise ratio and thereby the lowest error in estimating the standardised scenario. The resultant standardised scenario may be scaled for more "optimistic" emission scenarios (= lower emissions scenarios); the scaling for more pessimistic emission scenarios (= higher emissions scenarios) than those used for estimating the standardised scenario is not recommended: this would imply extrapolation, which is loaded by much higher error.

Choice of the GCMs: Figure 2.2 shows the standardised scenarios for temperature and precipitation at Prague for 11 GCMs. The differences between scenarios derived from individual GCMs are due to differences in the GCMs (related to different parameterization of sub-grid phenomena, different spatial resolution, different representations of Earth surface, etc) and natural climate variability (the latter may be effectively modelled by the stochastic weather generator, which is linked to the climate change scenarios). To account for the inter-GCM variability in the given climate change impact analysis, we can either use scenarios from all available GCMs, or to use a subset of GCMs which consists of those GCMs which are among the best (in terms of the fit between observed climate and GCM-simulated climate) and represent the inter-model variability. Considering the amount of GCMs, we used a latter approach. Based on the earlier validation tests (Dubrovsky et al. 2005) the triplet of GCMs was used to define the standardised scenarios: HadCM3, ECHAM5 and NCAR-PCM, which satisfy the above conditions (simultaneously, the benefit of this triplet is that the chosen GCMs belong to the most frequently worldwide used GCMs, which allows comparison of results obtained with these scenarios with results of other authors.

The results for the Prague station show that the temperature will rise for all months of the year. The greatest increase will occur in winter and late summer. The precipitation is projected to significantly decrease in summer and early autumn. On the other hand, slight increase is probable to occur during the rest of the year.

Choice of the values of the scaling factor, ΔT_G: The increase in global mean temperature ΔT_G was estimated by one-dimensional energy-balance model MAGICC. To account for the uncertainties in climate sensitivity and emission scenarios, all possible combinations of the four marker emission scenarios (SRES-A1, SRES-A2, SRES-B1 and SRES-B2) and three values of climate sensitivity (low = 1.5 K, middle = 2.6 K, high = 4.5 K) were used to drive MAGICC while estimating the value of ΔT_G. Three of the 12 resultant values were used (found in the bottom line of the table): the LOW (highlighted in yellow colour) is the lowest of the four values related to the low climate sensitivity and 4 emission scenarios, the MIDDLE (highlighted in blue) is the median of the four values related to the middle climate sensitivity, and the HIGH (highlighted in green) is the highest of the four values related to the high climate sensitivity.

Tab.2.1 The increase in global mean temperature (with respect to 1961-1990) for three values of climate sensitivity (low/mid/high: 1.5, 2.6, 4.5 K), four marker emission scenarios (SRES-A1, -A2, -B1, -B2), and three futures (2025, 2050, 2100). The low (optimistic), middle and high (= pessimistic) estimates of ΔT_G are given in the bottom row of the table (SUM)

	2025	2050
	low / mid / high	low / mid / high
SRES-A1	0.60 / 0.85 / 1.17	1.02 / 1.47 / 2.07
SRES-A2	0.56 / 0.80 / 1.10	1.03 / 1.48 / 2.08
SRES-B1	0.49 / 0.70 / 0.98	0.76 / 1.11 / 1.57
SRES-B2	0.53 / 0.75 / 1.05	0.84 / 1.22 / 1.73
SUM	**0.49** / **0.78** / **1.17**	**0.76** / **1.35** / **2.08**

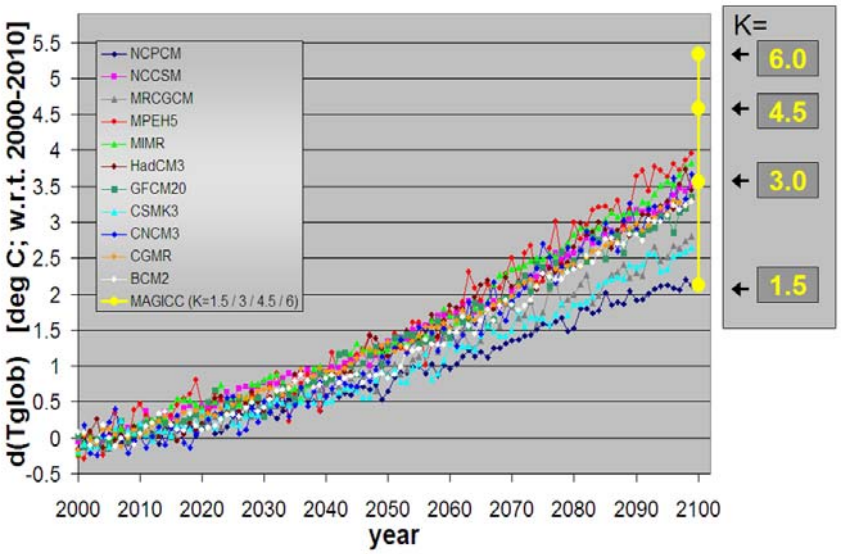

Figure 2.1 Increase of the global mean temperature according to 11 GCMs run under SRES-A2 scenarios and estimate of ΔT_G by MAGICC model (yellow dots) for the SRES-A2 emission scenarios and 4 values of the climate sensitivity (K).

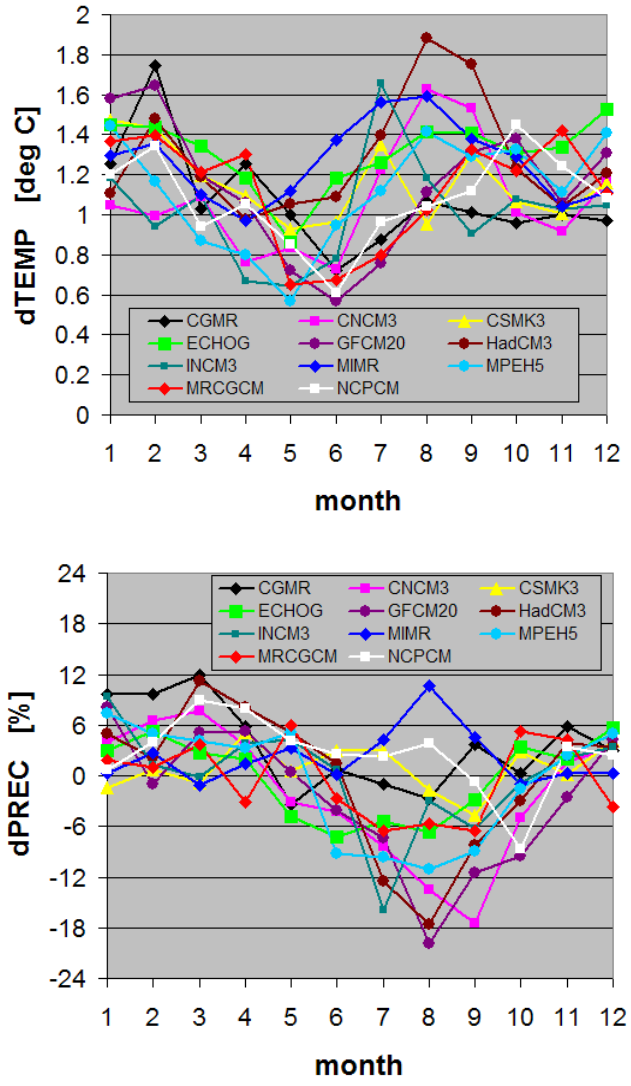

Figure 2.2 Standardised scenarios of changes in temperature (top) and precipitation (bottom) at Prague according to 11 GCMs run under SRES-A2 emission scenario. The changes relate to 1K rise in global mean temperature.

3. CUNI contribution

3.1. Introduction

Charles University's (CUNI's) contribution to the provision of climate change scenarios is based on the analysis of the outputs of the RegCM3 model, developed at the Abdus Salam International Centre for Theoretical Physics and run at CUNI. A description of the model and its integration domain is provided in the CECILIA deliverable D2.1; basic validation of the run driven by the ECHAM5 GCM, as well as simulated changes in mean temperature and precipitation for the periods 2021-2050 and 2071-2100, are presented in deliverable D2.6.

Along with scenarios based on raw outputs of the RegCM model, series subjected to postprocessing procedure, correcting for systematic errors in the statistical distribution of the target variables, were also used (these are referred to as postprocessed series in the following text). The corrective algorithm applied was based on the modified method of Piani et al. (2009); specific details are given in deliverable D3.2. The validation was carried out for the CECILIA common domain, covering parts of Austria, Czech Republic, Hungary and Slovakia – see deliverable D3.1 for specification of the domain and procedures used to generate the respective gridded datasets of observed values. The outputs of the RegCM model, both original and postprocessed, were IDW-interpolated onto the grid used by the set of observations in the CECILIA common domain.

The selected illustrative results here are presenting absolute or relative differences between the statistics of interest in the simulated climate for the period 2021-2050 and for the control period 1961-1990 (former minus/divided by the latter). For analogical analysis concerning expected changes in the period 2071-2100, see deliverable D3.5.

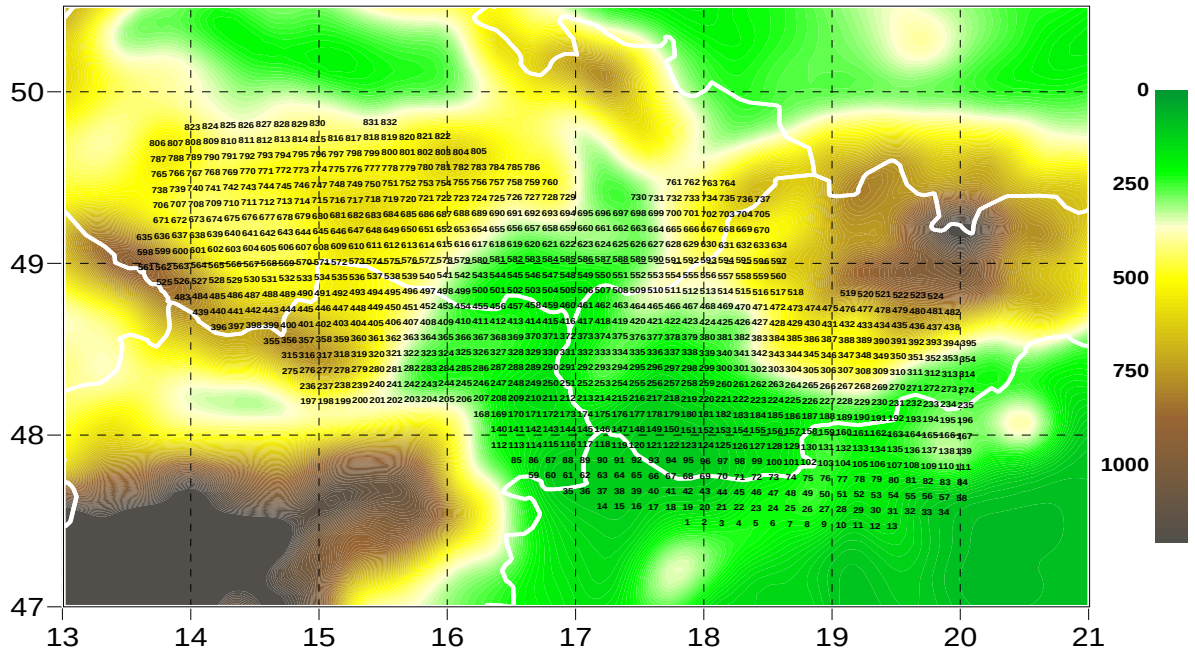

Figure. 3.1 Grid points of CECILIA common validation domain (identification numbers located over the respective gridboxes), drawn over the orography of the RegCM model (m)

The results are presented either in a form of maps covering the entire region of Central Europe (raw model outputs only) or graphs presenting the values of the analysed statistics for individual grid points of the validation domain shown in Fig. 3.1 (postprocessed data are shown along with their equivalents for unprocessed outputs of the RegCM model, to demonstrate the eventual contrast between the two). For analogical results derived for the period 2071-2100, see deliverable D3.5.

3.2. Changes of mean values of temperature and precipitation

The climate change signal is rather weak in Central Europe for precipitation in an annual average (Figure 3.2, left). Examining different parts of the year separately, the change is revealed to be rather small on average in DJF and JJA seasons and statistical postprocessing in the applied form does have little effect on its magnitude (Figure 3.3). A slight but systematic precipitation decrease was found for the MAM season. In the SON season, when the relatively highest increase was simulated, correction does further amplify it. This feature becomes even more evident for the period 2071-2100 (see deliverable D3.5).

The annual mean temperature increase of about 1°C was simulated in the CE domain (Figure 3.2, right). Similar increase was also typical for daily maximum and minimum temperature, annually as well as for individual seasons; postprocessing slightly amplifies the values derived from the raw model outputs (Figure 3.4). Postprocessing also brings additional spatial variability into the simulated fields of temperature increase, in contrast to the more geographically uniform values derived from raw model data.

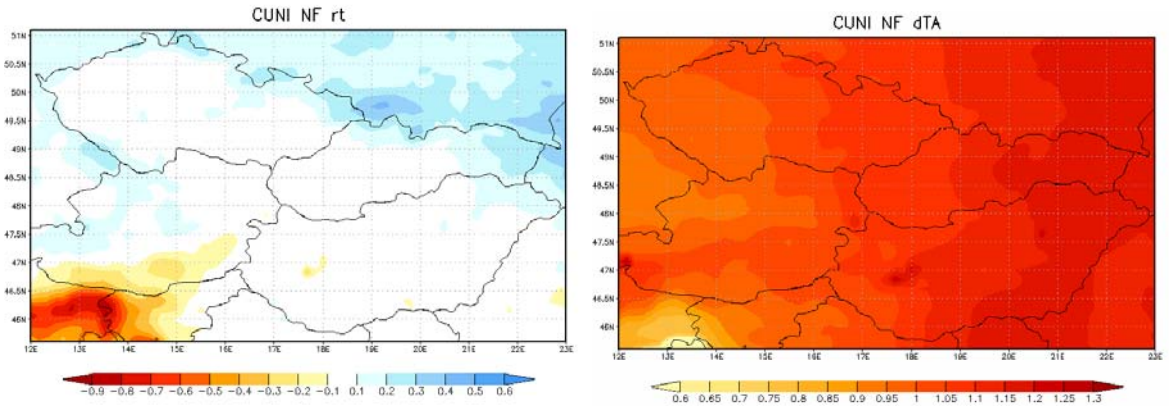

Figure 3.2 Absolute changes of precipitation (left, mm/day) and mean temperature (right, °C) in the CE region, for the period 2021-2050 relative to 1961-1990 (annual mean).

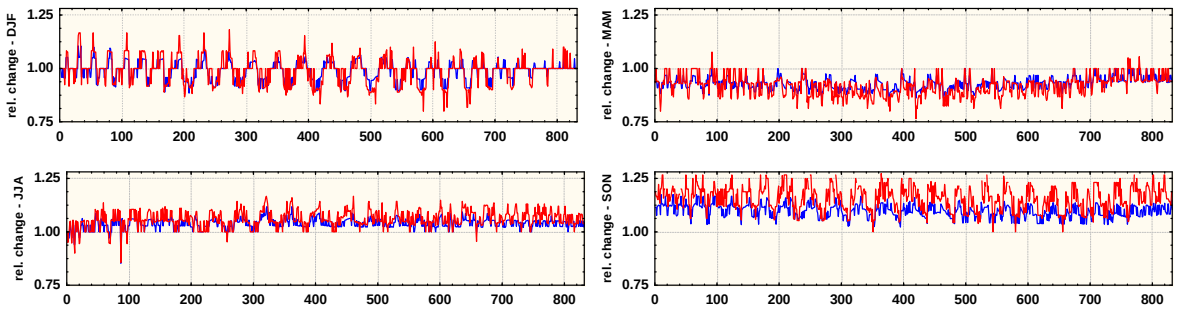

Figure 3.3 Precipitation change in different seasons, and the influence of postprocessing, for the period 2021-2050 relative to 1961-1990. Blue graph represents change in the original data, red in the postprocessed series; the horizontal axis shows identification numbers of the gridpoints in the validation domain.

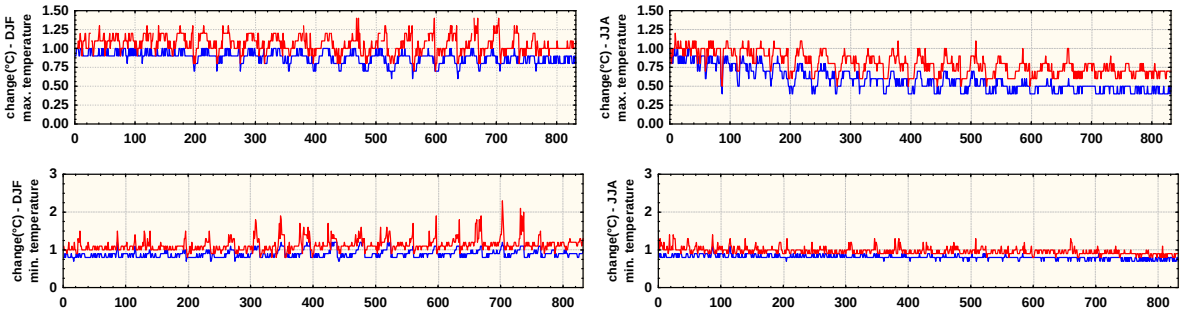

Figure 3.4 Maximum (top) and minimum (bottom) temperature change in DJF (left) and JJA (right) seasons, and the influence of postprocessing, for the period 2021-2050 relative to 1961-1990. Blue graph represents change in the original data, red in the postprocessed series; the horizontal axis shows identification numbers of the grid points in the validation domain.

3.3. Changes in the spread of values

While the signal describing future changes of variance is rather mixed for the temperature characteristics, a tendency for increase of precipitation variance (or other measures describing the spread of values) was found in most seasons, though this effect is still rather weak in the period 2021-2050. Postprocessing of the series changes the results very little with regard to the variance of daily data, as Figure 3.5 shows for the winter season.

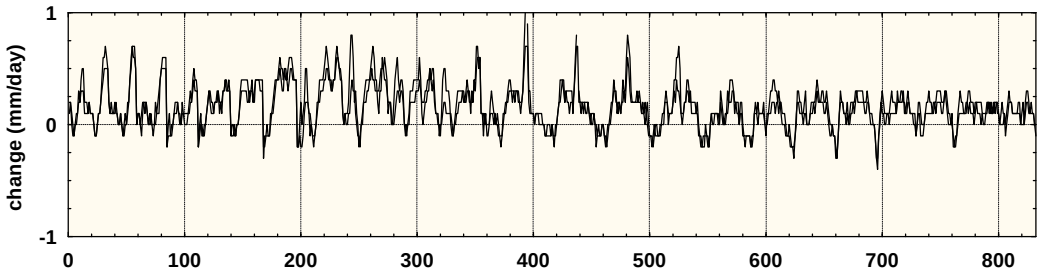

Figure 3.5. Change of standard deviation of daily precipitation sums in the DJF season, and the influence of postprocessing. Blue graph represents change in the original data, red in the postprocessed series; the horizontal axis shows identification numbers of the grid points in the validation domain.

3.4. Changes in the extreme tails of the statistical distributions

The changes of the values of the highest or lowest quantiles of daily temperature or precipitation do not precisely follow the evolution of mean values. In Figures. 3.6,7, 8, this is shown on selected examples, along with the effects of postprocessing. Note, for example, the strong increase for the 1% quantile of minimum daily temperature in winter (Figure 3.7), well above the rise of its mean value.

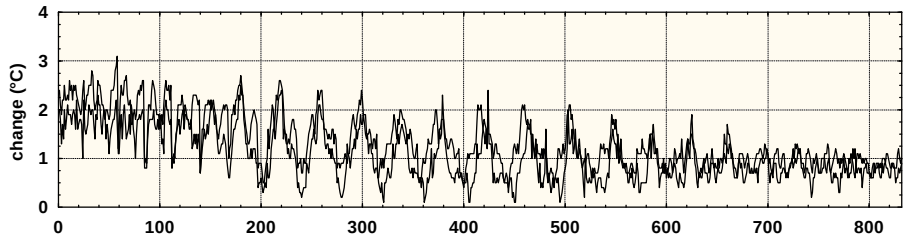

Figure 3.6. Changes of the value of the 99% quantile of maximum daily temperature, JJA season. Blue graph represents change in the original data, red in the postprocessed series; the horizontal axis shows identification numbers of the grid points in the validation domain.

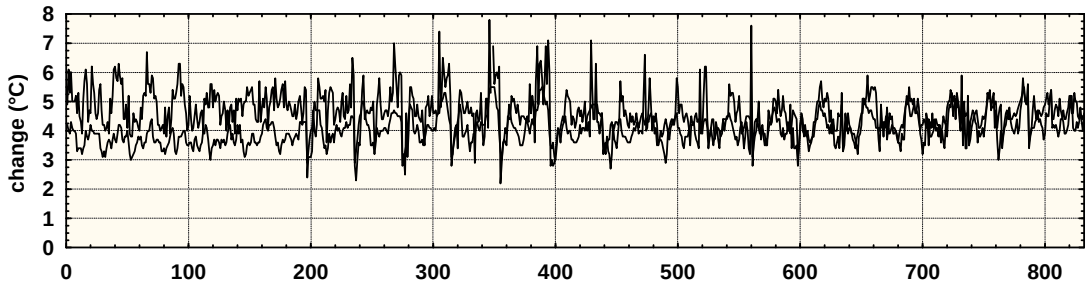

Figure 3.7 Changes of the value of the 1% quantile of minimum daily temperature, DJF season. Blue graph represents change in the original data, red in the postprocessed series; the horizontal axis shows identification numbers of the grid points in the validation domain.

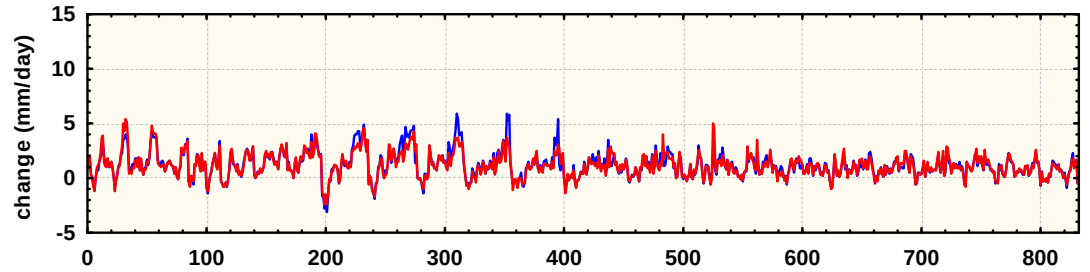

Figure 3.8. Changes of the value of the 99% quantile of daily precipitation, DJF season. Blue graph represents change in the original data, red in the postprocessed series; the horizontal axis shows identification numbers of the grid points in the validation domain.

3.5. Changes of special derived characteristics

Influence of the simulated climate change on selected characteristics related to the frequency of (non)exceedance of characteristic values of temperature or precipitation is shown for a few selected examples in this section. There seems to be a mild tendency towards increase of heavy precipitation events in summer (Figure 3.9). There is an increase of the number of tropical days (maximum temperature over 30°C), shown in Figure 3.10. Another distinct effect of the simulated climate change is the drop in the number of winter days when temperature does fall under the freezing point (Figure 3.11).

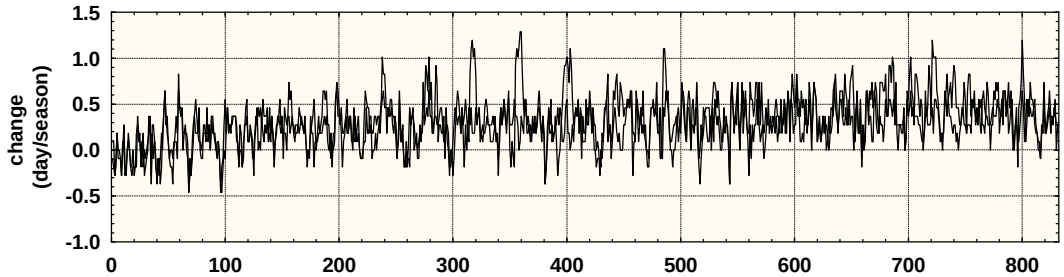

Figure 3.9 Change of the number of days with precipitation over 20 mm in JJA season. Blue graph represents change in the original data, red in the postprocessed series; the horizontal axis shows identification numbers of the grid points in the validation domain.

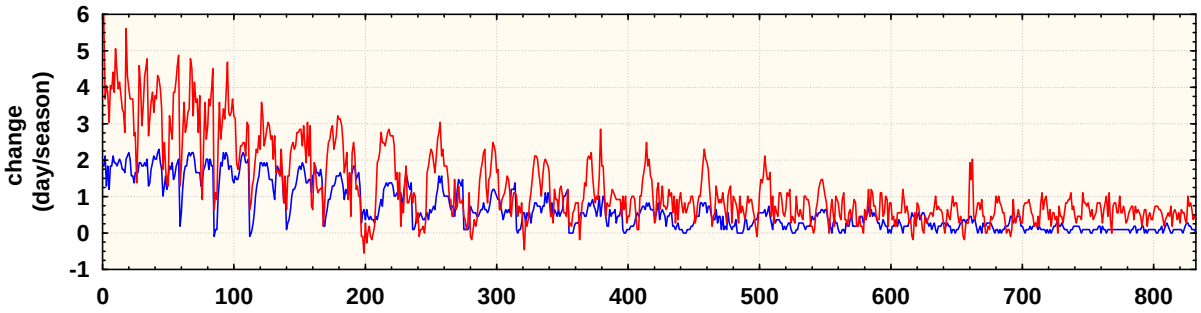

Figure 3.10 Change of the number of days with maximum temperature over 30 °C in JJA season. Blue graph represents change in the original data, red in the postprocessed series; the horizontal axis shows identification numbers of the grid points in the validation domain.

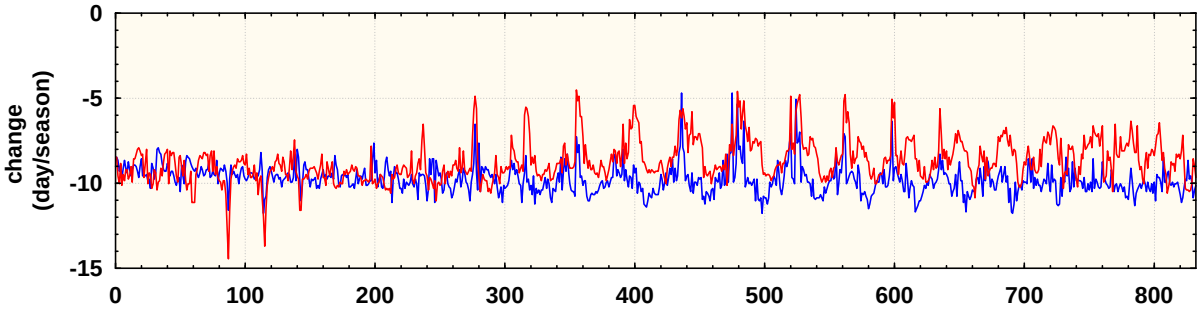

Figure 3.11 Change of the number of days with minimum temperature below 0 °C in DJF season. Blue graph represents change in the original data, red in the postprocessed series; the horizontal axis shows identification numbers of the grid points in the validation domain.

4. NMA contribution

4.1. Methodology overview

The statistical downscaling models (SDMs) used by the NMA in the CECILIA project are based on the canonical correlation analysis (CCA) technique (Von Storch et al., 1993, Busuioc et al., 1999, 2006). These models have been developed for the mean temperature (94 stations covering the entire Romania) and precipitation total (16 stations covering a southeastern area, used for the impact studies in CECILIA). In a previous work (Busuioc et al., 2006) has been found that, in case of precipitation, it is difficult to find a single skilful SDM for the entire Romanian area, due to the complex Romanian topography. More skilful SDMs can be found over smaller regions. Therefore, the SDMs developed by NMA in the CECILIA project refer to a smaller area (Figure 4.1) used for impact studies presented in the WP5 and WP6.

Compared to previous studies, when the SDMs have been mainly developed on seasonal scale, taking into account the necessities of the impact studies, these models have been developed on monthly scale. According to the CCA techniques presented in previous papers (Busuioc et al., 1999, 2006), the inputs in the SDM (predictors and predictands) are considered as anomalies projected on the EOF (empirical orthogonal functions) space, retaining the time series associated to the most important EOFs, which explain the most part of the observed variance, used then as inputs in the CCA. In the frame of CECILIA project, the monthly anomalies are considered together, stratified on the four seasons (DJF, MMA, JJA and SON) for precipitation and on cold (November to April) and warm (May to October) seasons in case of temperature.

The temperature field at 850 mb (T850) has been considered as predictor for temperature while the sea level pressure (SLP), geopotential heights at 500 mb (H500) and specific humidity at 850 mb (separately or in combination)

have been tested as predictors for precipitation. It has been found that the SDMs for temperature present a high and stable skill while for precipitation, even if the skill is significant, the magnitude of the observed anomalies is not always very well reproduced. More details about the SDM validation are presented in the deliverable D.3.3.

In order to obtained the scenarios for the time slices 2021-2050 and 2070-2099, the skilful SDMs calibrated over the period 1961-1990 have been applied to the GCM outputs from 8 ENSEMBLES GCMs (stream1 simulations, http://cera-www.dkrz.de/WDCC) under the A1B emission scenario. The ARPEGE outputs have also been used for the temperature scenarios until now, but only for the time slice 2070-2099 (see D3.5). The GCMs used as inputs in the SDMs are: EGMAM (FUB) -3 runs, ECHAM5 -3 runs, BCM2 and INGV. The ensemble mean of the SDM projections based on these GCM outputs have been calculated in order to reduce the uncertainties. The full range of the SDM projections for all GCM inputs is also presented. The results for the time slice 2021-2050 are presented in the following.

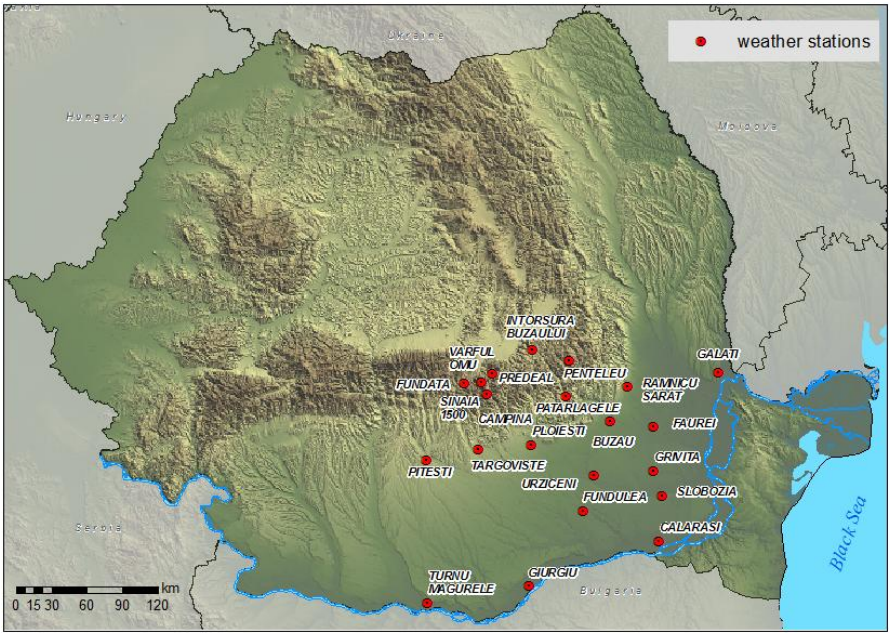

Figure 4.1 The location of the stations used in developing the SDMs for precipitation.

4.2. Change in the mean temperature

Figure 4.2 shows the temperature changes at the 94 Romanian stations represented as ensemble mean of the 8 SDM projections, averaged for each season (winter, spring summer and autumn). It can be seen that the highest values are obtained for summer (between 1.2^0C and 1.9^0C) with the highest magnitude over the southern-southwestern regions. For the other seasons, a similar climate signal has been obtained (changes between 0.8^0C and 1.5^0C) with the highest magnitude over the northwestern regions. This ensemble averages represents the most likely value from the considered SDS projections but there are large differences from one projection to another, depending on the driver GCM. In Table 1 the spatial average over Romania for various SDs projections is presented, showing that, ***over the period 2021-2050, under the A1B scenario, it expected a temperature change ranging between 0.6^0C and 1.9^0C (mean 1.0^0C) for winter, between 0.5^0C and 1.7^0C (mean 1.1^0C) for spring, between 1.2^0C and 2.1^0C (mean 1.6^0C) for summer and between 0.7^0C and 1.8^0C (mean 1.4^0C) for autumn.*** This result is in agreement with those obtained from the ensemble mean of 7 ENSEMBLES GCMs, except for winter when the SDS signal is lower (Figure 4.3). An example about the spatial pattern of temperature change in summer derived from the RCM simulations (ensemble average) is presented in Figure 4.4. A more reliable comparison has been made between SDMS driven by the ECHAM5-run 3 and three

ENSEMBLES RCMs driven by the same GCM (details in Figure 4.3). It can be seen that there are differences between the RCM signals, the SDS signal being included between RCM ranges and it is more similar with the MPI-REMO signal, except for winter.

It is known that the SDS credibility is dependent also by the performance of the driver GCM in projection of change in the predictor. It is very difficult to assess the future projections, the only way being the assessment of GCM performance in simulating the predictor variability under the current climate conditions. In figure 4.5, the difference between the T850 spatial average derived from the GCM current climate simulations and corresponding observed (reanalysis) values. The ECHAM5 GCMs reproduce the best the current T850 conditions as magnitude (figure 4.4) and spatial patterns (given by the spatial correlations, not shown), The FUB GCMs underestimate the summer values and the INGV overestimate them.

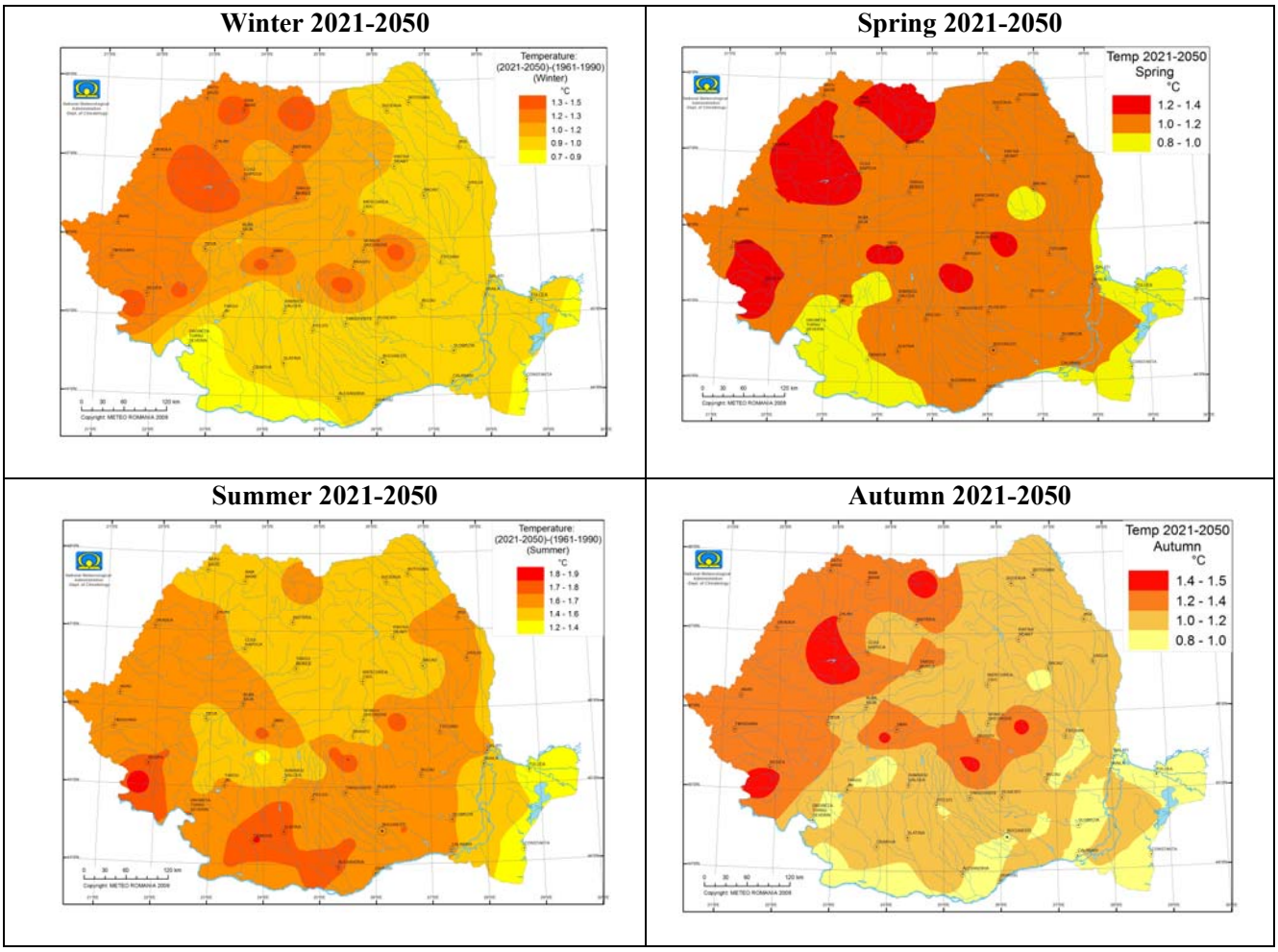

Figure 4.2 Change of the seasonal temperature mean (2021-2050 vs. 1961-1990) under the A1B emission scenario at 94 stations in Romania (^{o}C), represented as ensemble mean over SDM projections from the 8 ENSEMBLE GCM simulations (stream 1).

.

Table 4.1 Spatial average (over 94 stations) of the monthly temperature change in Romania for the 2021-2050 against 1961-1990, under A1B scenarios derived from the SDM projections driven by various GCMs.

	BCM2	EH5-1	EH5-2	EH5-3	FUB1	FUB2	FUB3	INGV
Winter	0.7	0.6	1.0	0.7	1.6	1.0	1.9	0.9
Spring	1.1	0.5	1.3	1.0	1.7	1.2	1.0	0.8
Summer	1.8	1.5	1.7	1.4	1.6	1.2	1.4	2.1
Autumn	1.0	1.5	1.8	1.7	1.4	0.7	1.6	1.3

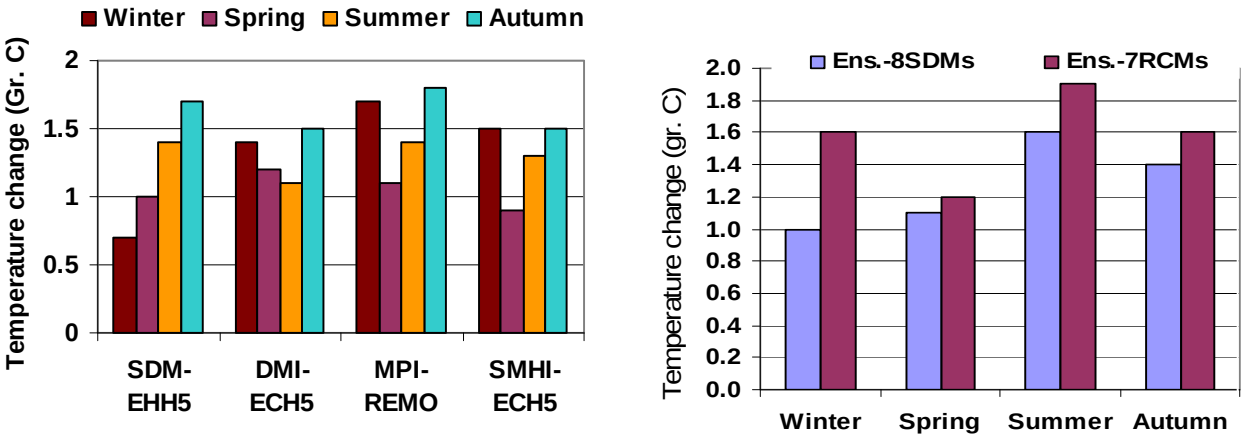

Figure 4.3 Change of the seasonal mean temperature (2021-2050 vs. 1961-1990) averaged over Romania derived directly from various ENSEMBLES RCMs and indirectly through SDM, driven by the ECHAM5-3 (left). On the right, the ensemble mean of the 8 SDM projections in comparison with the ensemble mean of 7 RCMs.

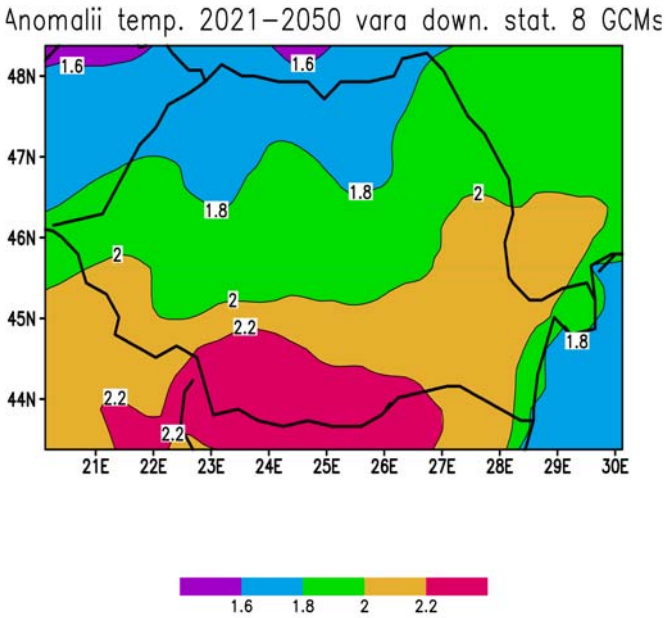

Figure 4.4 Change of the summer temperature mean (2021-2050 vs. 1961-1990) under the A1B emission scenario represented as ensemble mean over 7 ENSEMBLES RCMS.

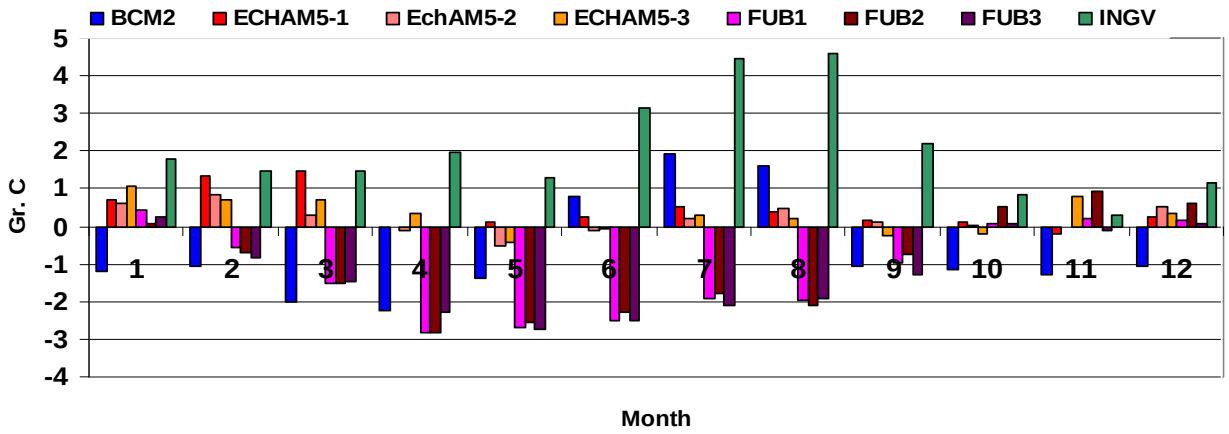

Figure 4.5 Differences between the monthly means of T850 (^{o}C) derived from observations (reanalysis) and ENSEMBLES GCM simulations (stream 1): 1961-1990.

Precipitation change

As it has been presented in the deliverable D3.3, the sea level pressure field covering the area 10-45^{0}E, 30-55^{0}N was found as the best predictor for precipitation in all the seasons (DJF, MAM, JJA, SON), with the highest skill for winter and lower for summer. Even if, the SDM does not reproduces always very well the magnitude of the observed precipitation anomalies, the temporal evolution and the long term mean is quite well reproduced. This result has been proved by the reconstruction of the monthly precipitation anomalies over the independent data set 1991-2007 with the model fitted over the period 1991-1990. It was found that the observed change in monthly precipitation over 1991-2007 compared to 1961-1990 is well reproduced by the SDM (more details in the deliverable D3.3).

The optimum model for each season (optimum combination of EOFs/CCAs) has been applied to the SLP changes for two time slices (2021-2050 and 2070-2099) derived from 8 GCMs (ENSEMBLES, stream1, see section 4.1). The ensemble average has been computed and the results for the first time slice are presented in Table 4.2. The corresponding results for the 2070-2099 time slice are presented in the deliverable D3.5. The climate signal is similar from one SDM projection to another, apart from the magnitude, giving some robustness to the results (see Table 4.3). It can be concluded that, ***under the A1B scenario, the precipitation is likely to slightly decrease in winter months over the entire region and over plain area in some other months. Not significant change is generally expected during the spring, summer and autumn, except for some increase in May.***

In order to express better the uncertainty associated to the SDS signal, the spatial average of the seasonal SDS signal derived from the projection using the ECHAM5-3 driver, has been compared to the corresponding signal derived from three RCMs driven by the same GCM, including their average (Figure 4.6). It can bee seen that the two signals are the most similar for summer. This result is in agreement with those obtained in the ENSEMBLE project (van der Linden and Mitchel, 2009) and presented in the IPCC AR4 (IPCC, 2007), showing that the summer signal is coherent between various RCM, GCMs over the southern Europe, that gives more robustness to this result. The SDS signal is also in agreement with the results obtained by the high resolution RegCM (10 km) simulations presented in WP2.

The added value of the SDS technique is its capability to be easily applied to outputs from various GCM experiments (being computationally inexpensive), that allows to assess the uncertainty of regional climate change estimations.

Table 4.2 Change of monthly precipitation (%) at 16 stations from the southeastern Romania derived as ensemble average over SDM projections from 8 ENSEMBLE GCM: 2021-2050 vs. 1961-1990, A1B scenario.

Station	Winter			Spring			Summer			Autumn		
	XII	I	II	III	IV	V	VI	VII	VIII	IX	X	XI
Câmpina	-16	-17	-18	-17	-6	5	-6	-2	-2	-4	-9	-6
Călăraşi	-8	-11	-13	-6	-3	6	-12	-11	-8	-4	-8	-6
Fundata	-6	-9	-11	-8	-4	6	-2	0	0	-6	-8	-11
Fundulea	-11	-15	-15	-13	-6	6	-14	-10	-10	-3	-10	-7
Giurgiu	-11	-12	-15	-1	1	12	-11	-6	-4	-4	-10	-6
Griviţa	-10	-14	-13	-15	-7	5	-13	-10	-7	-5	-12	-8
Int. Buzăului	-4	-7	-11	-7	-5	5	-6	-3	-3	-5	-8	-14
Piteşti	-13	-15	-17	-14	-4	8	-9	-5	-7	-5	-10	-7
Ploieşti	-14	-16	-18	-19	-7	6	-9	-5	-4	-3	-10	-6
Predeal	-8	-9	-12	-8	-5	6	-5	-4	-4	-6	-8	-12
Rm. Sărat	-15	-14	-14	-12	-4	7	-9	-5	-5	-4	-13	-7
Sinaia	-14	-12	-16	-18	-6	5	-2	1	1	-6	-8	-7
Târgovişte	-14	-14	-17	-17	-6	6	-10	-7	-9	-5	-11	-7
Tr. Măgurele	-11	-12	-15	0	2	13	-10	-2	0	-4	-10	-5
Urziceni	-11	-14	-13	-24	-10	5	-13	-11	-8	-4	-10	-8
Vf. Omu	-3	-10	-10	3	-4	2	-5	-1	0	-5	-6	-13

Table 4.3 Spatial average (over the 16 stations presented in Table 4.2) of monthly precipitation change (%) derived from the SDM projections driven by various ENSEMBLE GCMs (stream 1): 2021-2050 vs. 1961-1990, A1B scenario.

	Winter			Spring			Summer			Autumn		
DriverGCM	XII	I	II	III	IV	V	VI	VII	VIII	IX	X	XI
BCM2	-25	2	-30	-15	0	6	-5	-9	13	0	-9	-17
EH5-1	13	-29	-21	19	7	-3	-16	2	-11	-5	-10	-30
EH5-2	-21	-22	-8	21	-5	2	-2	-11	-13	3	-39	-1
EH5-3	16	-19	0	-35	-10	17	-8	-4	-6	6	-1	24
FUB-1	-17	1	-18	-17	2	7	-15	-12	-4	-7	6	0
FUB-2	-23	-4	-14	-33	-11	21	-4	-6	-8	-20	-7	-15
Fub-3	-12	-9	-9	-11	-11	-8	-21	-1	-13	-18	-13	-9
INGV	-16	-19	-14	-17	-7	7	3	2	7	6	-1	-17

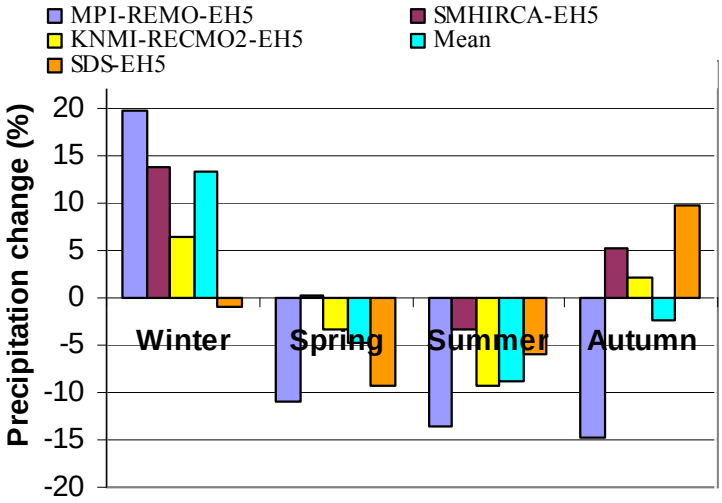

Figure 4.6 Spatial average of the seasonal precipitation change (%) over the area 24-27E, 43-45N covering the 16 stations presented in figure 4.1, derived from three ENSEMBLES RCMs and SDS driven by the EHAM5-3 GCM. The RCM average (mean) is also presented.

5) ELU Contribution

Introduction

The applied stochastic downscaling method has two key elements. The first element includes large-scale circulation of the atmosphere and the second element represents a linkage between local surface variables and large-scale circulation. The linkage is expressed by a stochastic model using an observational data series. Then, this model may be utilized with GCM outputs characterizing atmospheric circulation (Mearns et al., 1999).

Stochastic downscaling methods are based on the fact that there is considerable stochastic relationship between the large-scale atmospheric circulation and the meteorological, hydrological (hydrometeorological) variables. This relationship is estimated from observed data and then is used with large-scale circulation available from GCM output. Thus, estimation can be obtained for local meteorological and hydrometeorological parameters under a new warmer climate. (Bogárdi et al., 1993). The model was developed and applied for the Carpathian Basin. Computations were carried out using ECHAM driven RegCM regional climate model outputs (25 km horizontal resolution).

Evaluation of precipitation is a much more complicated task than temperature since it has a spatial-temporal intermittence (Bartholy et al., 1995). Therefore, it is necessary to analyze both the probability of precipitation occurrence and its magnitude in wet periods.

Stochastic downscaling methodology in the frame of CECILIA project

First, the stochastic downscaling technique was applied using the ERA-40 datasets for the period 1961-1990. As it is mentioned above, the method is based on the fact that there is considerable stochastic relationship between the large-scale atmospheric circulation and the meteorological variables (e.g., temperature and precipitation). This relationship was estimated from observed data (i.e., ERA-40 datasets) and then is used with large-scale circulation available from GCM/RCM outputs. Thus, estimation is obtained for local meteorological parameters under new climate conditions.

Large-scale circulation is characterized by macrocirculation (MCP) types of AT-700 hPa geopotential height data (at 00 UTC) for the region covering the following region with 325 (= 13x25) grid points: 35°-65°N, 30°W-30°E. The MCP types are defined using cluster analysis on a seasonal basis to the corresponding meteorological variables,

i.e., temperature or precipitation grid point time series for the region covering Hungary (4x8 = 32 grid points, lat-long: 46°-49°N, 16°-23°E).

Analysis

The statistical downscaling technique was applied for the Carpathian basin using the scenario experiments of RegCM for 3 time slices: 1961-1990, 2021-2050, 2071-2100. AT-700 hPa geopotential height data (at 00 UTC) from the ECHAM-driven RegCM experiments with 25 km horizontal resolution served as the predictor variable for the region covering the previously defined large-scale region. Gridded temperature and precipitation fields for the region covering Hungary (32 grid points, lat-long: 46°-49°N, 16°-23°E) were generated using the downscaling technique, and compared to the results of the RegCM experiments using 10 km horizontal resolution (and using the same 25 km horizontal resolution ECHAM-driven RegCM simulations that provided input fields for the stochastic model). Results of the 2021-2050 period are presented in this deliverable.

List of the analyzed parameters:
1. Coded large-scale circulation 40 types (10 types/season)
2. Seasonal averages of cluster centers (AT-700 hPa)
3. Time series of daily codes (1961-1990, 2021-2050, 2071-2100) – seasonal frequency distribution (Figure 5.1.)

Temperature
1. Seasonal mean change (Figure 5. 2a)
2. Seasonal change of standard deviation (Fig. 5.2b)

Precipitation
1. Seasonal mean (Figure 5.3a.)
2. Seasonal standard deviation
3. Seasonal mean on wet days only (Figure 5.3b.)
4. Seasonal frequency of wet days (Figure 5. 4.)

Summary of the results of the stochastical-dynamical downscaling model for 2021-2050, A1B scenario using RegCM model simulations for Hungary: only small changes are expected in temperature and precipitation conditions as it is shown in Figures 5.2-5.4.

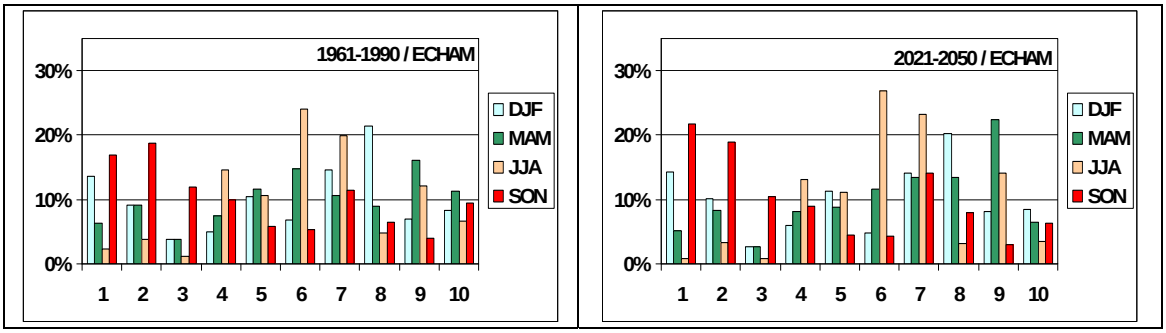

Figure 5.1: Seasonal distribution of MCP types using the ECHAM-driven simulation fields for 1961-1990 and 2021-2050.

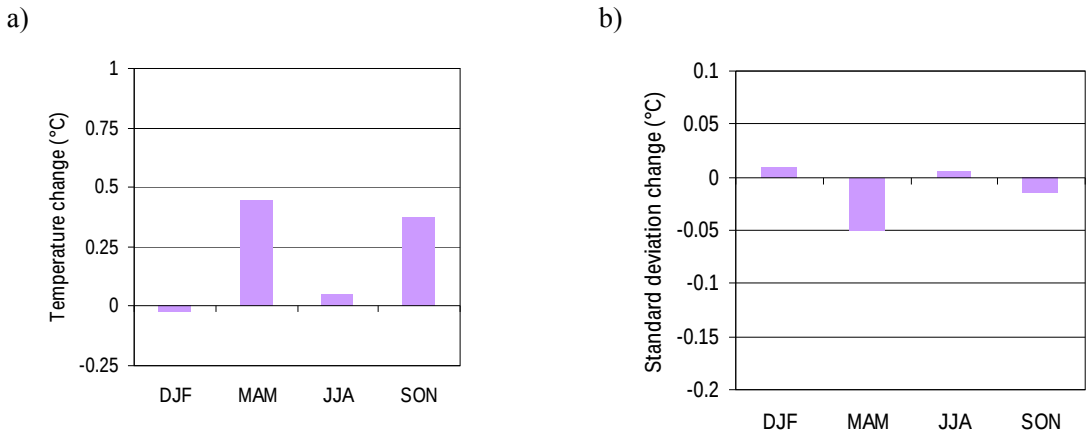

Figure 5.2: Spatial average of seasonal mean simulated temperature change (a) and standard deviation change of simulated temperature (b) for Hungary, for 2021-2050 relative to 1961-1990.

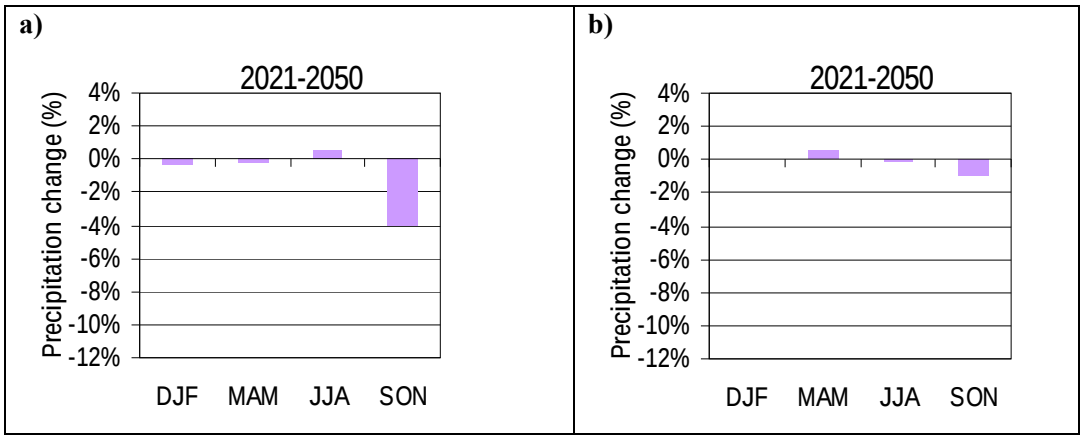

Figure 5.3: Spatial average of seasonal mean change of simulated precipitation (a) and of simulated wet-day precipitation (b) for Hungary, for 2021-2050 relative to 1961-1990.

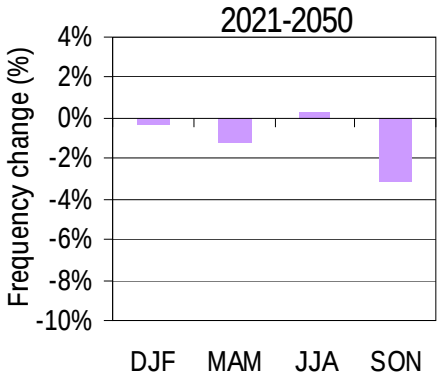

Figure 5.4: Spatial average of seasonal mean simulated frequency change of precipitation days (R > 1 mm) for Hungary, for 2021-2050 relative to 1961-1990.

References

Bartholy, J., Bogárdi, I., Matyasovszky, I., 1995: Effect of climate change on regional precipitation in lake Balaton watershed. Theor. Appl. Climatol. 51, 237-250.

Bogárdi, I., Matyasovszky, I., Bárdossy, A., Duckstein, L., 1993: Application of a space-time stochastic model for daily precipitation using atmospheric circulation patterns. J. Geophys. Res., 98(D9), 16,653-16,667.

Busuioc A, von Storch H, Schnur R (1999) Verification of GCM generated regional seasonal precipitation for current climate and of statistical downscaling estimates under changing climate conditions. J Climate 12**:** 258-272 .

Busuioc, A, F. Giorgi, X. Bi and M. Ionita, 2006: Comparison of regional climate model and statistical downscaling simulations of different winter precipitation change scenarios over Romania. Theor. Appl. Climatol.,86, 101-124. von Storch H, Zorita E, Cubasch U (1993) Downscaling of global climate change estimates to regional scale: An application to Iberian rainfall in wintertime. J Climate 6: 1161-1171.

Dubrovsky M., Zalud Z. and Stastna M., 2000: Sensitivity of CERES-Maize yields to statistical structure of daily weather series. Climatic Change 46, 447- 472.

Dubrovsky M., Buchtele J., Zalud Z., 2004: High-Frequency and Low-Frequency Variability in Stochastic Daily Weather Generator and Its Effect on Agricultural and Hydrologic Modelling. Climatic Change 63 (No.1-2), 145-179.

Dubrovský M., Nemešová I., Kalvová J., 2005: Uncertainties in Climate Change Scenarios for the Czech Republic. Climate Research (v tisku).

Harvey LDD, Gregory J, Hoffert M, Jain A, Lal M, Leemans R, Raper SBC, Wigley TML, de Wolde J (1997) An introduction to simple climate models used in the IPCC Second Assessment Report: IPCC Technical Paper 2 (eds JT Houghton, LG Meira Filho, DJ Griggs, M Noguer), Intergovernmental Panel on Climate Change, Geneva, Switzerland, pp.50

Hulme M, Wigley TML, Barrow EM, Raper SCB, Centella A, Smith S, Chipanshi AC (2000) Using a climate scenario generator for vulnerability and adaptation assessments: MAGICC and SCENGEN Version 2.4 Workbook. Climatic Research Unit, Norwich, UK, pp.52.

Mearns, L.O., Bogárdi, I., Matyasovszky, I., Palecki, M., 1999: Comparison of climate change scenarios generated from regional climate model experiments and empirical downscaling. Special issue on new developments and applications with the NCAR Regional Climate Model (RegCM), J. Geophys. Res., 104(D6), 6603-6621.

Piani C, Haerter JO, Coppola E (2009): Statistical bias correction for daily precipitation in regional climate models over Europe. Theor Appl Climatol, in print

von Storch H, Zorita E, Cubasch U (1993) Downscaling of global climate change estimates to regional scale: An application to Iberian rainfall in wintertime. J Climate 6: 1161-1171

van der Linden P., and J.F.B. Mitchel (eds.) 2009: ENSEMBLES: Climate Change and its Impacts: Summary of research and results from the ENSEMBLES project. Met. Office Hadley Centre, FitzRoy Road, Exeter EX1 3PB, UK. 160pp.

IPCC, 2007: Contribution of Working Group I to the Fourth Assessment Report of the Intergovernmental Panel on Climate Change Solomon, S., D. Qin, M. Manning, Z. Chen, M. Marquis, K.B. Averyt, M. Tignor and H.L. Miller (eds.). Cambridge University Press, Cambridge, United Kingdom and New York, NY, USA, 996 pp.